

Quantitative analysis of group-specific brain tissue probability map for schizophrenic patients

Uicheul Yoon,^a Jong-Min Lee,^{a,*} B.B. Koo,^a Yong-Wook Shin,^b Kyung Jin Lee,^b In Young Kim,^a Jun Soo Kwon,^b and Sun I. Kim^a

^aDepartment of Biomedical Engineering, Hanyang University, Sungdong P.O. Box 55, Seoul 133-605, South Korea

^bDepartment of Psychiatry, Seoul National University College of Medicine, Seoul 110-744, South Korea

Received 14 September 2004; revised 22 January 2005; accepted 28 January 2005
Available online 7 April 2005

We developed group-specific tissue probability map (TPM) for gray matter (GM), white matter (WM) and cerebrospinal fluid (CSF) on the common spatial coordinates of an averaged brain atlas derived from normal controls (NC) and from schizophrenic patients (SZ). To identify differences in group-specific TPMs, we used quantitative evaluation methods based on differences in probabilistic distribution as a global criterion, and the mean probability and the similarity index (SI) by lobe as regional criteria. The SZ group showed more spatial variation with a lower mean probability than NC subjects. And, for the right temporal and left parietal lobes, the SI between each group was lower than the other lobes. It can be said that there were significant differences in spatial distribution between controls and schizophrenic patients at those areas. In case of female group, although group differences in the volumes of GM and WM were not significant, global difference in the probabilistic distribution of GM was more prominent and the SI was lower and its descent rate was greater in all lobes, compared with the male group. If these morphological differences caused by disease or group-specific features were not considered in TPM, the accuracy and certainty of specific group studies would be greatly reduced. Therefore, suitable TPM is required as a common framework for functional neuroimaging studies and an a priori knowledge of tissue classification. © 2005 Elsevier Inc. All rights reserved.

Keywords: Magnetic resonance imaging; Tissue classification; Probabilistic difference; Mean probability; Similarity index

Introduction

Probabilistic atlases are thought to provide information about the neuroanatomical complexity and inter-individual variability within a specific population in a common stereotaxic coordinate system. In particular, anatomical and geometric brain tissue probability map (TPM) can provide key information for func-

tional neuroimaging studies, indicating the structural or tissue homogeneity of the areas of significant functional activations (Momenan et al., 2004; Tomaiuolo et al., 1999). In these studies, probability maps derived from healthy control subjects were used to give a common framework for identifying disease-specific features.

To allow for the comparison of imaging studies across individuals, imaging data have to be spatially normalized. This process is generally based on data from healthy control subjects and therefore poses several problems in pathological populations because of abnormalities in brain morphology specific to neurodevelopmental or neurodegenerative processes (Toga et al., 2001). If these morphological differences caused by diseases were not considered in TPM, the accuracy and certainty of specific group studies would be greatly reduced. In addition, TPM is not a critical factor in tissue classification, but simply an initial estimate for that procedure (Ashburner, 2000; Cocosco et al., 2003; Kamber et al., 1995; Leemput et al., 1999a,b). However, the more similar the morphology of the subject is to the average of the population represented by the TPM, the better the utility of the entire classification procedure (Cocosco et al., 2003). In fact, voxel-based morphometry (VBM), developed for automated unbiased analysis of structural magnetic resonance imaging (MRI) scans, demonstrates the essential problem with this approach: MRI scans of patients may have a different geometry than those of healthy controls. This is seen, for example, in patients with Alzheimer's disease, who show mainly ventricular enlargement and displacement of structures (Ashburner, 2000). As a result, healthy controls will match the standard template better than patients; especially near strong intensity gradients, there is a risk of measuring structure displacement on top of atrophy (Bookstein, 2001). Recently, several researchers have proposed an optimized VBM that used a study-specific local group template and TPM for further improvements to minimize error while maximizing sensitivity (Good et al., 2001a,b; Karas et al., 2003). Therefore, suitable TPM is required as a common framework for functional neuroimaging studies and an a priori knowledge of tissue classification.

* Corresponding author. Fax: +82 2 2296 5943.

E-mail address: ljm@hanyang.ac.kr (J.-M. Lee).

URL: <http://cna.hanyang.ac.kr>.

Available online on ScienceDirect (www.sciencedirect.com).

Most recent studies have used large archives of volumetric MRI scans to detect structural alterations in patients with schizophrenia. These show enlarged lateral and third ventricles (Lawrie and Abukmeil, 1998); reduced brain volume with disproportionate temporal lobe reductions and gray matter deficits (Csernansky et al., 1998; Lawrie and Abukmeil, 1998); thalamic and midline anomalies (Andreasen et al., 1994); hippocampal volume deficits and shape deformity (Csernansky et al., 1998; Lee et al., 2004; Wang et al., 2001); loss or reversal of cortical pattern asymmetry (Bilder et al., 1994; Falkai et al., 1992; Shenton et al., 1992). In this study, we developed group-specific TPMs for gray matter (GM), white matter (WM) and cerebrospinal fluid (CSF) on the common spatial coordinates of an averaged brain atlas derived from healthy controls and from schizophrenic patients.

We aimed to address the question of how substantially different is the TPM of schizophrenic patients from that of the normal population. With similar rationale, several other researchers have presented various methods for evaluating probabilistic results. Wilke et al. (2003) proposed differences in the distribution of tissue probability as the method of comparing pediatric and adult data. Although global differences can be shown by this visual inspection, it is deficient in quantitative comparisons of the probabilistic distribution in the specific brain region. Amunts et al. (1999) described a technique to quantify inter-individual spatial variability of Brodmann's areas using probability maps: that is, to compare the 50% probability volume with the mean volume of that area. In addition, Park et al. (2004) compared the probability maps for specific brain regions between healthy controls and schizophrenic patients by the relative 50% probability volumes and cumulative distributions of probability. Although these parameters can be assessed with voxel-wise comparisons of local areas by the use of statistical probability difference maps, it is necessary to present objective and quantitative measures representing the differences in spatial probability distribution in specific regions and the whole brain. In this study, we proposed quantitative evaluation methods for identifying differences in group-specific TPM, which show the differences in probabilistic distribution as a global criterion and the mean probability and the similarity index by lobe as specific regional criteria. This study was intended not to introduce a methodology for making any atlas or probability map, but to

Table 1
Demographic characteristics of the subjects

Characteristic	Schizophrenia (N = 59)		Healthy control (N = 59)		Student <i>t</i> test	
	Mean	SD	Mean	SD	<i>t</i>	<i>p</i>
Age (years)	27.32	5.62	26.07	5.32	-1.25	0.22
Male (N = 36)	28.08	5.33	26.58	5.72	-1.15	0.25
Female (N = 23)	26.13	5.97	25.26	4.63	-0.55	0.58
Education (years)	14.17	2.51	15.54	1.87	3.37	<0.01
Estimated IQ ^a	100.63	15.14	116.37	9.70	6.73	<0.01
Parental SES ^b	3.02	0.82	2.97	0.72	-0.36	0.72
SES	3.24	0.73	2.69	0.56	-4.52	<0.01
PANSS ^c total score	66.81	17.37				

^a Intelligence quotient.

^b Socioeconomic status, from the highest as 1 to the lowest as 5.

^c Positive and negative symptom syndrome scale.

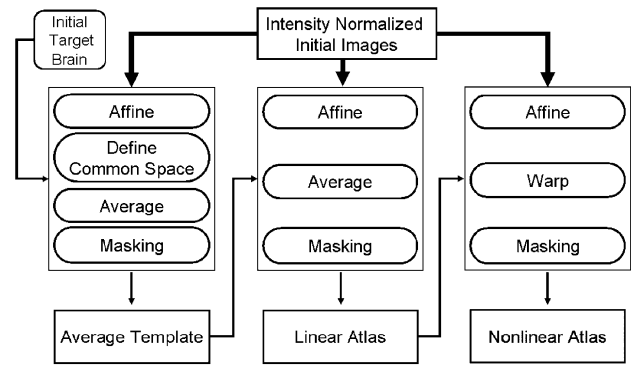


Fig. 1. The procedure for producing an average brain atlas as a common spatial coordinate. The thick arrows indicate the flow of all images, and the narrow arrows indicate a single image. The whole procedure consists of three steps. First, the averaged template (AVT) was constructed as a *bias-free* registration target. Then, linear registration was performed based on the AVT for global scaling and linear alignment. Finally, nonlinear fifth-order polynomial warping was completed to eliminate natural variations caused by the non-rigidity of brains in vivo.

evaluate the spatial variation of each tissue of the brain in schizophrenia using probabilistic maps.

Materials and methods

Subjects

A group of right-handed schizophrenic patients was recruited from the inpatient unit and the outpatient clinic at Seoul National University Hospital, Seoul, South Korea. Fifty-nine patients (36 male, 23 female) were interviewed with the Structured Clinical Interview for DSM-IV (SCID-IV) and met those criteria for schizophrenia. Exclusion criteria for patients were any lifetime history of neurological or significant medical illnesses and any past history of substance abuse. Each patient's symptoms were rated on the Positive and Negative Syndrome Scale (PANSS; Kay et al., 1987). The normal control group was recruited from Internet advertisements and consisted of 59 healthy subjects matched for age, sex, handedness and parental socioeconomic status (SES) with the patients group. Exclusion criteria for controls were any current or lifetime history of DSM-IV axis I disorder. The demographic characteristics of patients and controls are summarized in Table 1. Although there were no significant group differences in these characteristics between schizophrenia and comparison subjects in mean age (27.32 ± 5.62 vs. 26.07 ± 5.32 years) and parental SES (3.02 ± 0.82 vs. 2.97 ± 0.72), the numbers of years of education, estimated IQ and personal SES did differ significantly (Table 1). The mean PANSS total score of the patients was 66.81 ± 17.37 . This study was carried out under guidelines for the use of human subjects established by the institutional review board. All subjects gave written informed consent for the procedures before their participation in the study (Kim et al., 2003; Kwon et al., 2003). To assess group-specific differences in our results, we divided our sample into male and female subgroups for analysis.

MR image acquisition and preprocessing

MR images were acquired using a 1.5 T GE SIGNA scanner (GE Medical System, Milwaukee, WI, USA) using a 3D-SPGR

T1-weighted spoiled gradient echo pulse sequence with the following parameters: 1.5 mm sagittal slices; echo time 5.5 ms; repetition time 14.4 ms; number of excitations 1; rotation angle 20°; field of view 21 × 21 cm; matrix 256 × 256 voxels.

Following previous studies (Kim et al., 2003; Lee et al., 2003), images were resampled to be isocubic and realigned so that the

anterior–posterior axis of the brain was aligned parallel to the inter-commissural line and the other two axes were aligned along the inter-hemispheric fissure. The data sets were then filtered using 2D affine anisotropic diffusion filtering to improve the signal-to-noise ratio. These procedures were processed using the commercial software ANALYZE 4.0 (Mayo Foundation, USA).

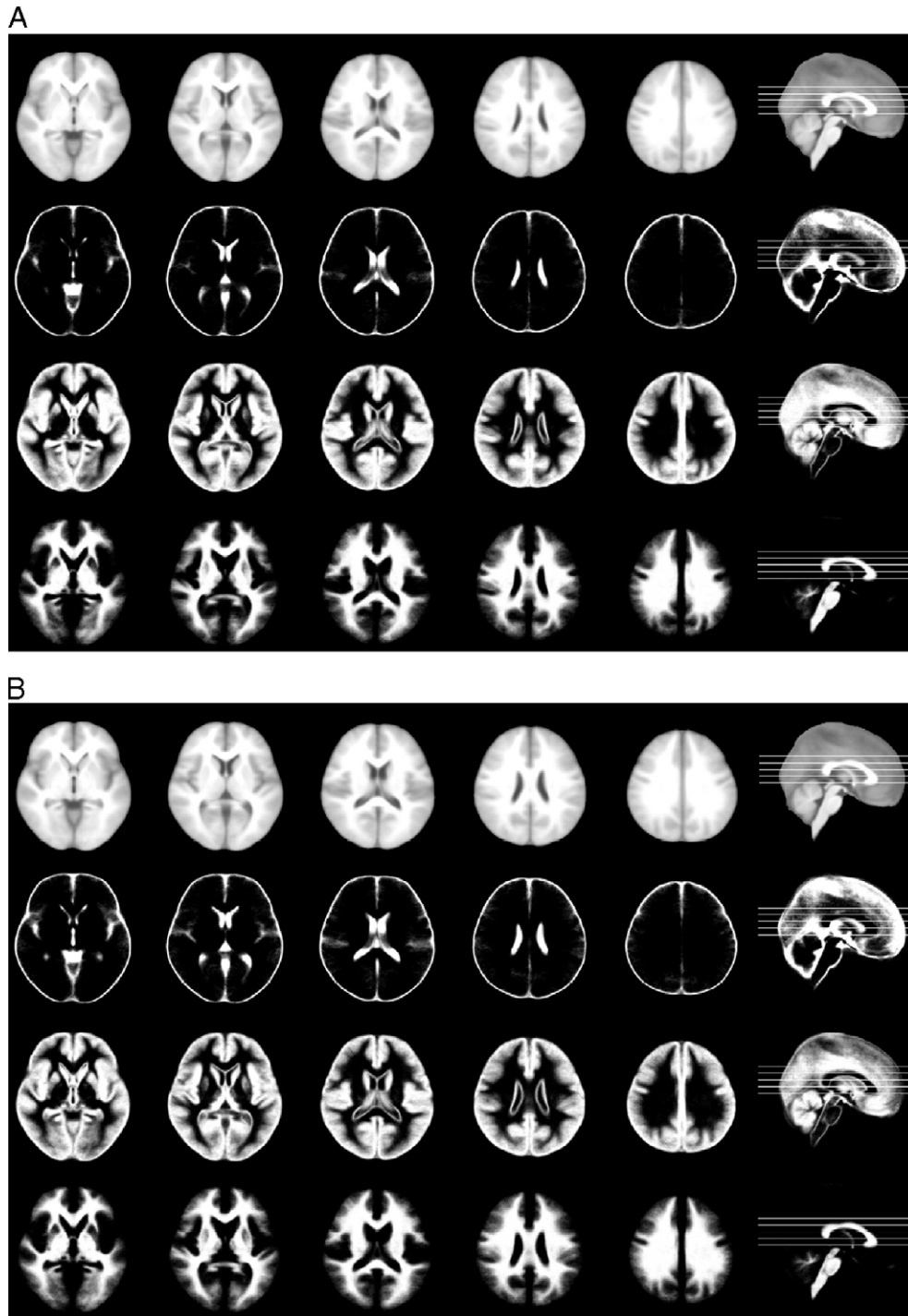


Fig. 2. Tissue probability map (TPM) derived from (A) normal control (NC) population and (B) schizophrenic (SZ) patients. Although the average brain atlas of the NC group was similar to that of the SZ group, there were more enlarged ventricles and greater atrophy of cortical gray matter in the patients with schizophrenia.

Skull stripping and tissue classification

Non-brain tissue components of the images were removed by the modified region-growing method (Lee et al., 2003). We applied morphological operations to the extracted cerebral image to restore the peripheral CSF approximately in the sulcus, but not in the gyrus. These operations consisted of sequential dilation, to expand the image, and erosion, to shrink it. The extracted cerebral images were classified into GM, WM and CSF, using a fuzzy clustering algorithm that was chosen because it did not require the use of a priori probability (Yoon et al., 2003). Total intracranial and global tissue volumes and the volume ratio of GM to WM before the processing for TPM were calculated to compare differences in probability distribution.

Intensity averaged brain atlas as a common spatial coordinate

We constructed two average brain atlases derived from healthy controls and schizophrenic patients as the common spatial coordinates for group-specific TPM. The *Automated Image Registration Tool* (AIR, version 5.2.5) was used for the linear and nonlinear registration (Woods et al., 1998a,b). The original procedure was derived and modified from ‘AIR Make Atlas’ pipeline, proposed by Rex et al. (2003). The process consists of three construction steps (Fig. 1): the average template (AT), the linear atlas (LA) and the nonlinear atlas (NA). First, all intensity-normalized images were affined to a randomly selected subject within a group that was visually inspected to screen out severe abnormalities to reduce variations of global position and scale and averaged to make the AT. To avoid the subsequent registration procedure from being biased by using an individual image as a registration target, these affine transforms are averaged to define a “least distant space” for every subject to be transformed into and the AT was used as the registration target for the LA. Then, the voxels of intensity under a pre-defined threshold on the boundary were masked out to form the AT. The whole images were affined to the AT and averaged and masked again, yielding the LA. Finally, to construct the NA, all volumes were affined and warped onto the LA followed by averaging and masking. For this step, non-rigidity of the brain was assumed using nonlinear fifth-order polynomial warping. The NA was thus produced from the intensity averaged brain images.

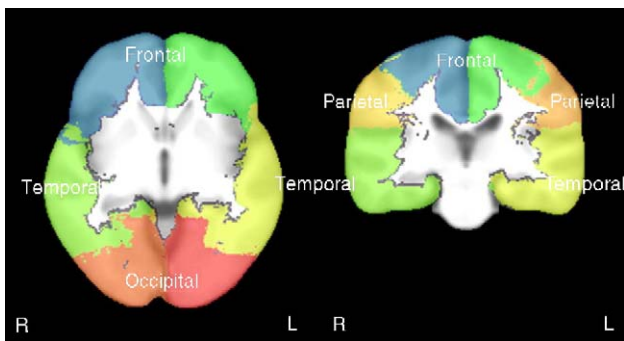


Fig. 3. Maximum probability maps for the average brain atlas. They are used to divide the probability map of gray matter into the frontal, temporal, parietal and occipital lobes.

Table 2
Results of volume measures

	Group	Volume (cm ³)		Statistics	
		Mean	SD	<i>t</i>	<i>Sig.</i>
Intracranial volume	NC	1543.358	135.048	-0.05	0.96
	SZ	1544.426	121.430		
	NC_M	1608.082	119.244	0.94	0.35
	SZ_M	1583.825	98.995		
	NC_F	1442.051	88.747	-1.24	0.22
	SZ_F	1482.758	129.489		
CSF	NC	179.926*	54.094	-4.79	<0.01
	SZ	227.794*	54.505		
	NC_M	191.418*	60.429	-2.50	0.02
	SZ_M	224.513*	51.418		
	NC_F	161.937*	36.750	-4.85	<0.01
	SZ_F	232.930*	59.839		
Gray Matter (GM)	NC	845.501*	76.669	2.21	0.03
	SZ	816.225*	66.599		
	NC_M	877.849*	68.844	2.64	0.01
	SZ_M	838.349*	57.250		
	NC_F	794.869	59.704	0.73	0.47
	SZ_F	781.374	66.317		
White Matter (WM)	NC	518.615	49.144	2.01	0.05
	SZ	500.372	49.343		
	NC_M	539.935	44.110	1.80	0.08
	SZ_M	520.779	45.982		
	NC_F	485.244	36.928	1.56	0.13
	SZ_F	468.431	36.153		
GM/WM	NC	1.634	0.099	-0.23	0.82
	SZ	1.639	0.134		
	NC_M	1.630	0.103	0.36	0.72
	SZ_M	1.619	0.147		
	NC_F	1.641	0.094	-1.01	0.32
	SZ_F	1.670	0.106		

There were no differences in the volume ratios of gray matter and white matter, although there were significant group differences in the volumes of cerebrospinal fluid and gray matter, but not in the white matter or intracranial volumes.

* NC: normal control, SZ: schizophrenia; W: whole, M: male, F: female.

Tissue probability map

All subjects were spatially normalized to the corresponding averaged brain atlas. Derived transform parameters were then applied to the tissue-classified volume of each subject. Averaging the normalized tissue volumes across subjects created a probability map at each voxel. The probability for any specific tissue at a given voxel described the percentage of subjects in which this particular voxel was classified to that tissue. For example, if a voxel with a coordinate (x, y, z) was classified as GM for only 1 out of 10 subjects, its probability of belonging to GM was assigned 0.1. The group-specific TPM for each subpopulation, such as all normal controls (NC, TPM_NC), all patients with schizophrenia (SZ, TPM_SZ), NC males, NC females, SZ males and SZ females, was constructed and evaluated for group-specific features in structural differences in their probability distributions (Fig. 2). For the voxel-wise comparison between groups, the average brain atlas of the SZ group was affine transformed into that of the NC group to

remove possible differences in global size and shape. This derived transformation matrix was then applied to the tissue volume of SZ and a new TPM_SZ, realigned to the average brain atlas of the NC group, was reconstructed.

Evaluation of probabilistic distribution

To account for different image contrasts caused by different field strengths and field inhomogeneities, results were only considered valid if the difference in tissue probability distribution

was found to be larger than 20% at a given voxel. For visualization of probability differences between groups, the difference in each voxel was color-coded and superimposed on the TPM_NC, used as a background image.

Although there was global dissimilarity between TPMs, as shown by probability differences, the maximum probability map by lobe was applied to identify regional differences between GM probability distributions. Although most procedure of maximum probability map followed the approach of Hammers et al. (2003), neuroanatomically trained investigator delineated man-

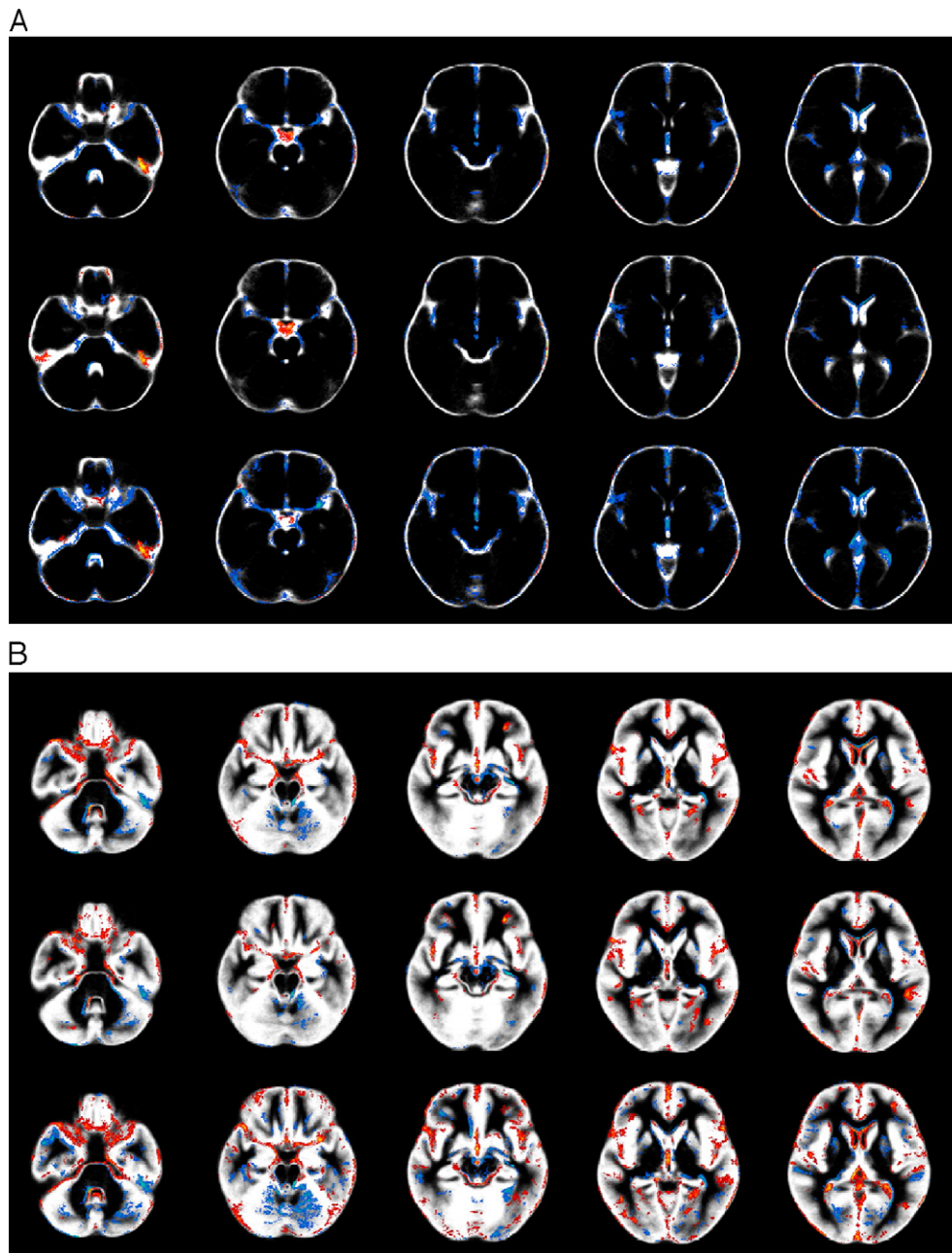


Fig. 4. Results of extracting differences between group-specific TPMs of the whole (top), males (middle) and females (bottom). (A) Cerebrospinal fluid, (B) gray matter and (C) white matter. Blue represents a higher tissue probability in the schizophrenic patient than the normal control population, with red indicating the opposite effect. The software MRlcro was used to display the image and to set the minimum cluster size to 100 voxels (<http://www.mricro.com>).

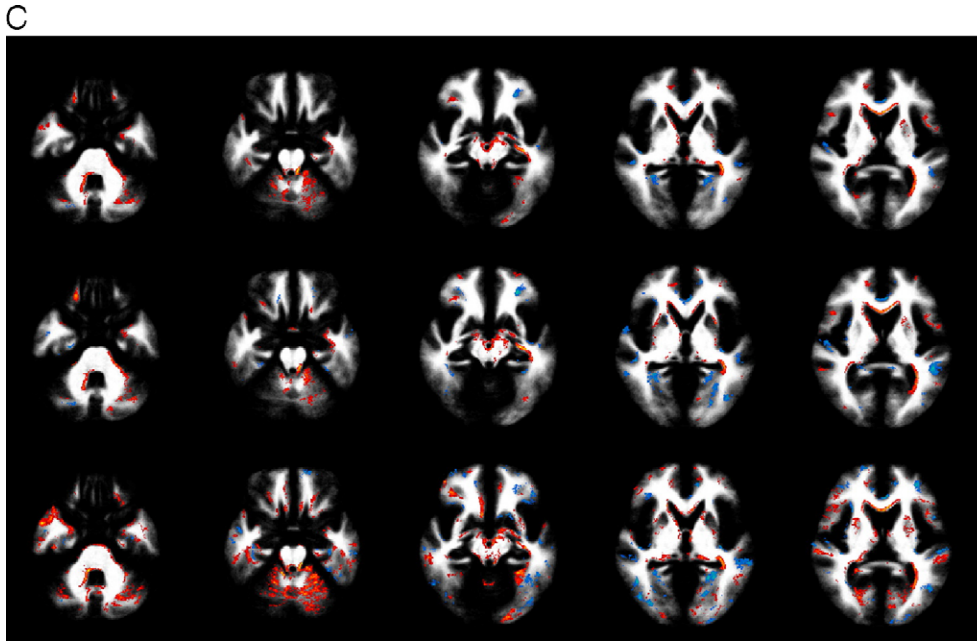


Fig. 4 (continued).

ually subdivisions of the brain using ANALYZE 4.0 (Mayo Foundation, USA). The definition of boundary between lobes in the manual parcellation has been described in the published literatures (Caviness et al., 1996; Crespo-Facorro et al., 1999; Kim et al., 2000; Rademacher et al., 1992). For frontal lobe, there are major landmarks to define boundaries (Crespo-Facorro et al., 1999). On the medial wall: (1) above the body of the corpus callosum (CC), an imaginary vertical line dropped from the point where the central sulcus intersects with the midsagittal plane (Rademacher et al., 1992); (2) below the genu of the CC, an imaginary vertical line passing through the most anterior tip of the inner surface of the genu of the CC. On the lateral surface, the posterior boundary is the central sulcus (or Rolando's fissure). The lateral, medial, anterior, superior and inferior boundaries of the frontal lobe are defined by its natural limits. The callosal sulcus constitutes the inferior boundary of the frontal lobe on the medial wall of the hemisphere. For temporal lobe, 6 major temporal sulci—Heschl's sulcus, first transverse sulcus, superior temporal sulcus, inferior temporal sulcus, occipitotemporal sulcus and collateral sulcus—and 7 artificial coronal slices were used to define medial/superior or lateral/inferior borders of temporal subregions (Kim et al., 2000). These subregions were merged to define whole temporal lobe. Remaining region that had not defined to frontal or temporal lobe was parcellated to occipital and parietal lobe. Major landmarks were used to separate occipital and parietal lobe (Caviness et al., 1996): (1) plane including intraparietal fissure—transverse occipital fissure; (2) plane including anterior limit of calcarine fissure; (3) cuneal fissure—parietooccipital fissure; (4) cuneal point (calcarine fissure—parietooccipital fissure). The maximum probability map was constructed from the whole NC population in this study (Fig. 3).

The mean probability and corresponding *L/R* asymmetry for major lobes of each group were calculated, where *L* and *R* were measures for the left and right hemispheres. The mean

probability at a given voxel reflects the average spatial variability within each group. For example, if a voxel had a larger degree of spatial variability within its group, the mean probability might be decreased. The asymmetry index was also computed according to the expression $2 \times (L - R) / (L + R)$. The symmetry range was established between the index values -0.1 and $+0.1$ (Galaburda and Eidelberg, 1982; Shapleske et al., 1999). Asymmetrical cases, therefore, were those showing values below -0.1 (right-sided pattern) or above $+0.1$ (left-sided pattern).

In addition, binary segmentations in the GM probability map by lobe of each group were produced by applying different thresholds onto the probability map. Using these segmentations, the similarity index (SI) was calculated between groups for identifying the effect of spatial variability on probability map. Cocosco et al. (2003) showed experimentally that the false positives in TPM as a training set for the supervised classifier amounted to just about 3% of all selected locations for the highest probability threshold. It means that the spatial locations which have a higher probability represent the core pattern of structural distribution. Therefore, even though global similarities at a lower probability threshold are related generally to both volumetric differences and spatial variability, it can be said that the effect of spatial variability is more conspicuous than volumetric difference at a higher probability threshold. The SI was used to measure the similarity (*k*) of two sets as the ratio of the size of their intersection divided by the size of their union.

$$k(S_1, S_2) = \frac{2|S_1 \cap S_2|}{|S_1| + |S_2|}$$

These *k* values ranged from 0 for sets that have no common elements to 1 for sets that are identical (Zijdenbos et al., 1994).

Results

Global volume differences in segmented brain tissues

The statistical significance of differences between groups was assumed at $P < 0.05$. Although WM and intracranial volumes did not differ between the patients and the control subjects, the SZ group had significantly smaller GM and larger CSF volumes than the NC subjects, except for the GM value of the female groups (Table 2). However, there was no difference between groups in the volume ratio of GM to WM.

Global probabilistic differences between group-specific TPMs

Although the average atlases of the two groups appear to be similar, the TPMs differed (Fig. 2). Thus, visual inspection of Fig. 2 shows some cortical atrophy and enlarged ventricles in the SZ group. A detailed comparison is overlaid on the TPM_NC, with the color coding representing the direction of differences: red denotes a higher tissue probability in the NC group compared with the SZ group, and blue indicates the opposite (Fig. 4). This color-coded image represents at least a 20% difference in tissue probability and includes clusters of more than 100 voxels. In general, the SZ group showed a higher probability for CSF and a lower probability for GM, relative to the normal control. Compared with the distribution of GM and CSF probability differences at the same time, the relative decrease in probability of GM corresponded to the increase of probability in peripheral CSF and lateral ventricles of the patients with schizophrenia. Moreover, although group differences in the volumes of GM and WM were not statistically significant for females, these differences were more prominent, compared with the whole and the male groups. In particular, there was a reduction in the frontal areas and an increase in the probability image of GM in the

cerebellum of the female patients with schizophrenia, but this was not evident for the male patients (Fig. 4B).

Regional differences between group-specific GM probability maps

Fig. 5 shows the mean probabilities and corresponding L/R asymmetries for major lobes of each group of subjects. Whereas the mean probability of left occipital lobe amounted above 70% in all the groups, the mean probability of left frontal and right parietal lobes did not yet get to 60%. As with global differences, the mean probability of the NC group was greater than that of the SZ subjects in all lobes. Both male and female subjects with schizophrenia tended to show more spatial variability than the control subjects, indicated by lower mean probability. In particular, in both temporal lobes and left occipital lobe, the differences in mean probability between all groups marked over 3%. The female schizophrenic group had higher mean probability values than the male schizophrenic group in most parts of GM, except for both occipital lobes and right temporal lobe. However, it is difficult to conclude that spatial variation caused by the disease might be greater in males than in females for the schizophrenic patient because several other factors such as volumetric difference and morphological shape variation are also mixed in this mean probability. Although the control subjects showed a left-sided asymmetrical pattern of mean probability in the occipital lobe, this asymmetrical property tended to diminish in the patients with schizophrenia.

Fig. 6 presents the SI with the threshold running from 0.5 to 0.9, which was calculated between groups for identifying the effect of spatial variability on probability map. The SI between each group was lower in the right temporal and left parietal lobes than in other lobes. It could be said that there were significant differences in spatial distribution between the NC and SZ groups at those areas. Although the SI decreased as the threshold level increased,

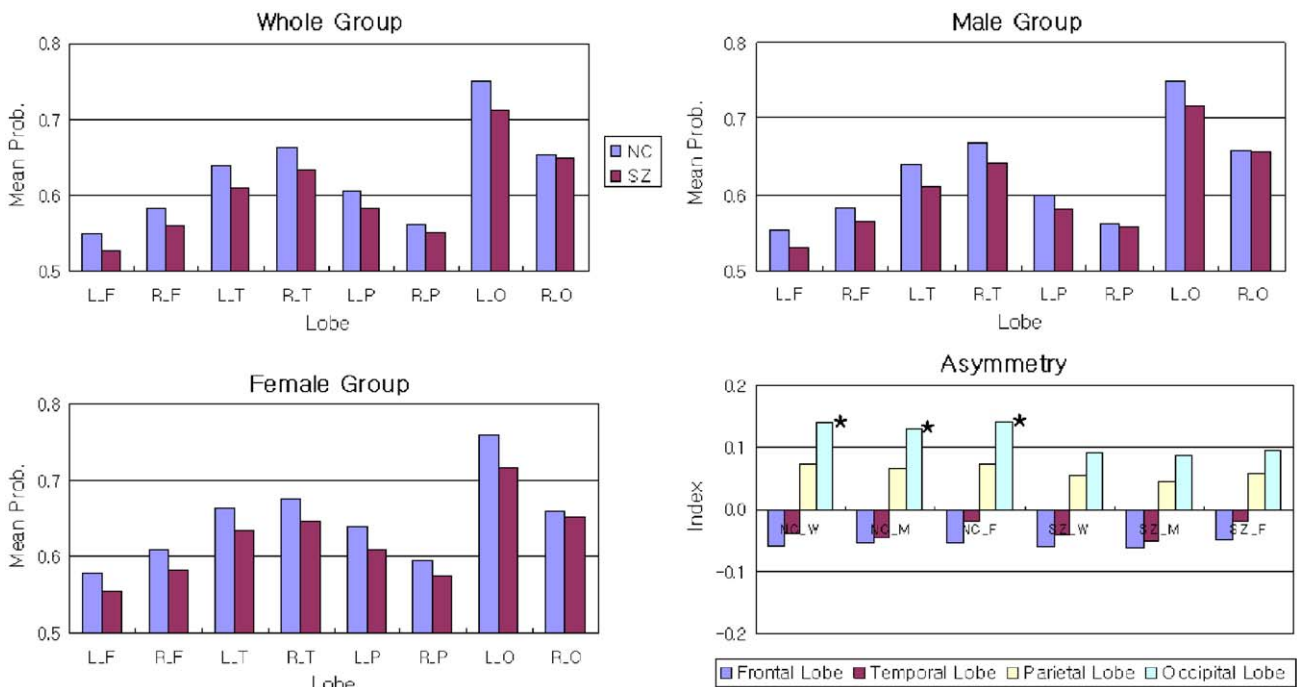


Fig. 5. Mean probability and asymmetry index of each lobe in the probability map for gray matter of each group. * L: left, R: right; F: frontal, T: temporal, P: parietal, O: occipital. ** NC: normal control, SZ: schizophrenia; W: whole, M: male, F: female. *** Symmetry range: -0.1 to +0.1.

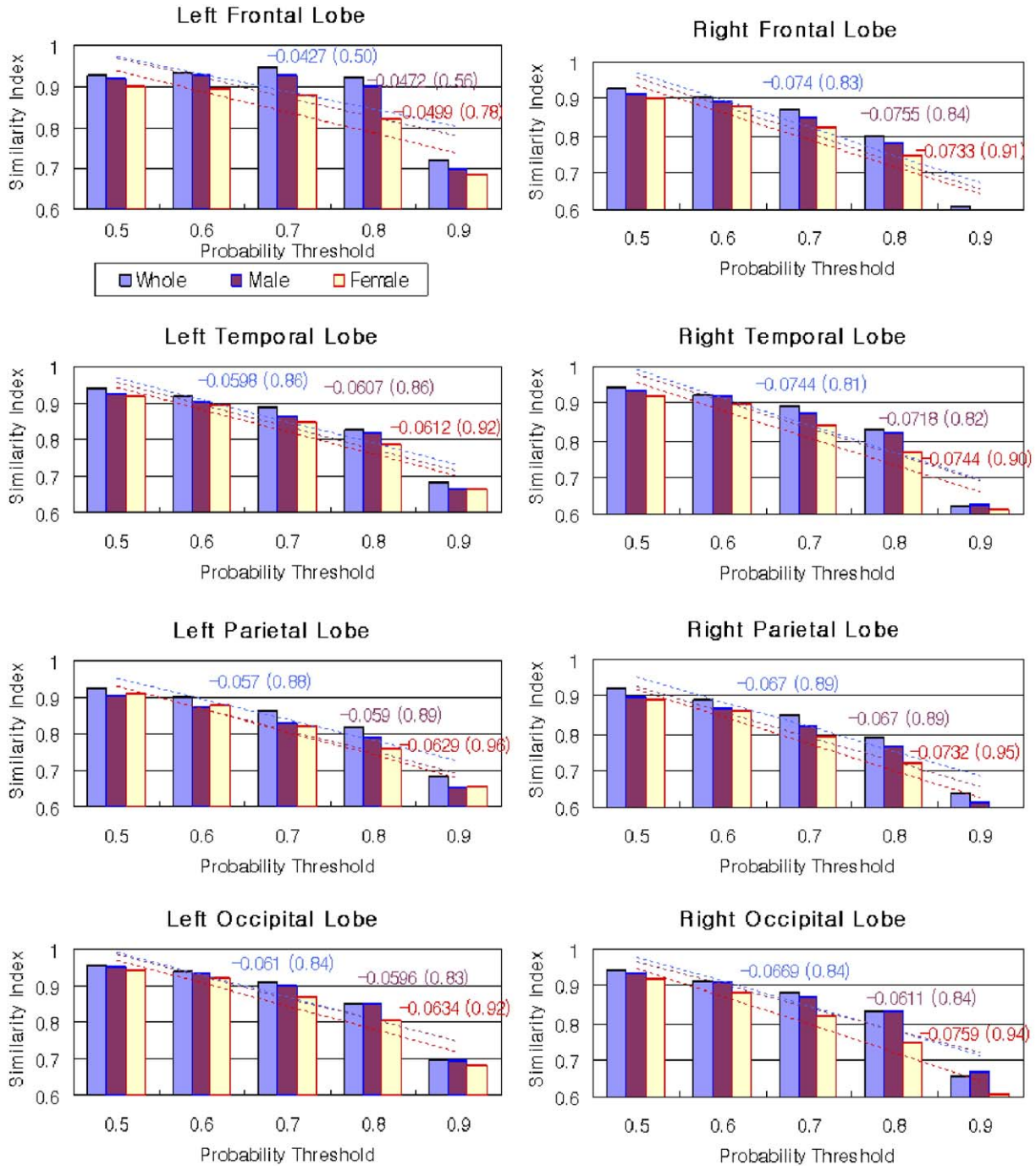


Fig. 6. Similarity index between the binary segmentations of each group with the probability threshold in each lobe. The index of females is relatively lower and its descent rate was greater in all lobes than for the other groups. The numbers indicate the correlation index and the square of the correlation coefficient which come from linear regression analysis.

its descent rate was different from each other in all lobes. In particular, the SI for the female group was lower and its descent rate was greater in all lobes, compared with the male group. For example, while the descent rate of SI in the female group was 7.6% ($R^2 = 0.94$) in the right occipital lobe, that of the male group was only 6.1% (0.84). It could be explained that the global difference in the probabilistic distribution of GM was more prominent in females and spatial variation caused by disease might be greater in females than in males for the schizophrenic patient.

Discussion and conclusion

Differences in probabilistic distribution for patients with schizophrenia

We found significant group differences in GM and CSF volumes, but not in WM volume, except for the female group in GM. This was consistent with several previous studies that demonstrated enlarged lateral ventricles and a global reduction

of GM volumes in patients with schizophrenia (Csernansky et al., 1998; Lawrie and Abukmeil, 1998; Wright et al., 2000). This is evident by simple visual examination of the global difference in probabilistic distribution. A global decrease of GM probability coincided with an increase of probability in the peripheral CSF and lateral ventricle of the patients with schizophrenia, relative to the control subjects. On the other hand, although the volume differences in GM and WM in females were not significant, there were greater differences in probabilistic distribution. It is not possible to conclude that the probabilistic distribution reflects only volumetric differences, because spatial variability and morphological deformation are also encoded in that probability. Because volumetric comparisons tend to underestimate the disease-specific abnormalities, such as spatial variations and morphological characteristics, it can be said that the probability at a given voxel might provide additional useful information when combined with conventional volume measures.

For regional differences, the mean probability of the SZ group was lower than that of the NC group in all lobes. The SZ group clearly showed significant differences in the pattern of spatial variation compared with the NC group. Park et al. (2004) suggested that schizophrenic subjects showed a significantly lower spatial overlap of specific brain region than controls, even after nonlinear spatial normalization, suggesting a greater heterogeneity in the spatial distribution of that area. They used a brain template based on healthy control subjects as a registration target for the patients. Although in this study the average brain atlas derived from schizophrenic patients was used as the common spatial coordinate of TPM_SZ with regard to a different morphology, there was still some anatomical variation between patient and control groups. Therefore, it should be noted that inconsistent registration within group could make a difference in the interpretation of functional neuroimaging (Brett et al., 2002).

In schizophrenia, structural brain abnormalities such as ventricular enlargement, volume reductions in the temporal lobe structures and anomalous cerebral asymmetries have been suggested to be greater in male patients than in female patients, contrary to the results of this study. However, Lawrie and Abukmeil (1998) reported that further studies were required in affected women to identify the clinical and etiological associations of those findings. Suzuki et al. (2002) observed GM reductions in the right prefrontal areas and increased regional GM in the parietal areas and the cerebellum in female patients, but not in male patients. In addition, Nasrallah et al. (1990) reported the frontal area to be significantly reduced in female patients with schizophrenia as compared with female controls, although they found no significant group differences in the frontal area in male subjects. In this study, we found that the probability of GM predominantly decreased in the frontal area and increased in the cerebellum in the female patients, but these trends were not remarkable in the male patients. And, for female subjects, the value of SI was lower and its descent rate was significantly greater in all the major lobes, compared with the male subjects. From our results and those of earlier studies, it may be assumed that male and female patients with schizophrenia have some different patterns of structural brain abnormalities. Therefore, a better group-specific TPM is required to minimize error while maximizing sensitivity of tissue classification, which represents morphology similar to the average of a given population.

Methodological considerations

The main contribution of this study is to evaluate the spatial variation of each tissue of the brain in schizophrenia using probabilistic maps. Although there have been many researches for morphological differences in schizophrenia from healthy control, this is the first study to investigate the spatial distribution of each tissue of the brain of schizophrenia using probabilistic map for whole brain, not a specific ROI. Unlike other voxel-based or ROI-based volume comparison methods, the proposed method was concentrated on the spatial variation within a group and compared these spatial variations between groups using similarity index. When combined with the volume-based studies, this kind of spatial variation analysis could give additional useful information to understand the morphological characteristic of schizophrenia's brain.

However, there are two limitations to this study. First, it was difficult to identify group differences in the probabilistic distribution of peripheral CSF regions. This arose from the morphological approximation in the skull-stripping procedure of image analysis. It is impossible to define exactly by visual inspection whether the cerebrum includes the entire CSF, because the intensity of CSF in T1-weighted MRI is similar to that of the background, despite manual establishment of the region of interest. Second, supplementary evaluation methods for probabilistic results are needed, apart from the visual inspection and other measures used in this study. We used the similarity index which is calculated between groups as an efficient way to overall evaluate the voxel-wise probabilistic difference. The change pattern of the similarity index according to probability threshold represents variability of structural distribution. In general, binary segmentation of the probability map, produced by applying different thresholds, is compared with the gold standard, which is produced via manual segmentation by an anatomist using a similarity index. In practice, the probability of voxels might be more useful than binary segmentation and it would be desirable to have a general measure for clarity of the evaluation representing the accuracy of the probability map as a whole. Anbeek et al. (2004) proposed a limited probabilistic similarity index, in which probabilistic outcomes were evaluated by comparison with binary references. Therefore, a probabilistic version of the similarity index that can be compared between probabilistic results is required.

Even excepting spatial variability, there can be other factors, such as registration error and segmentation error, in the probability map. Both of probability maps were generated by the same registration program and automated segmentation method was applied for identifying lobes from both of probability maps. Although there might be some errors, it can be assumed that those errors are removed mostly through the comparison between two maps. Actually, the purpose of this study was to identify the spatial variability caused by schizophrenia using the analysis of differences between probabilistic maps.

Conclusions

The extreme variability in the structural conformation of the human brain poses significant challenges for the construction of

population-based probabilistic atlases. Probabilistic atlases retain information on cross-subject variations in brain structure and function. These atlases are powerful tools with broad clinical and research applications (Kikinis et al., 1996; Roland and Zilles, 1994; Thompson et al., 2000; Toga et al., 2001). Based on well-characterized patient groups, these atlases contain composite maps and visualizations of structural variability, asymmetry and group-specific differences. This quantitative framework can be used to recognize anomalies and label structures in new patients. Because they retain information on group anatomical variability, disease-specific atlases are a type of probabilistic atlas specialized to represent a particular clinical group. The resulting atlases can identify patterns of altered structure or function and can guide algorithms for knowledge-based image analysis (Dinov et al., 2000; Pitiot et al., 2002).

In conclusion, we have presented a procedure for constructing group-specific TPM and the quantitative evaluation methods of group-specific features in the structural differences of TPM. In particular, TPM from schizophrenic patients showed different spatial distributions in both global and regional aspects than in normal controls. These group-specific TPM results will be useful for the a priori knowledge of tissue classification and in the interpretation of functional activation and promise to improve the accuracy of group analysis.

Acknowledgments

This research was supported by a grant (M103KV0100-1403K220101420) from Brain Research Center of the 21st Century Frontier Research Program funded by the Ministry of Science and Technology of the Republic of Korea.

References

- Amunts, K., Schleicher, A., Burgel, U., Mohlberg, H., Uylings, H.B., Zilles, K., 1999. Broca's region revisited: cytoarchitecture and intersubject variability. *J. Comp. Neurol.* 412 (2), 319–341.
- Anbeek, P., Vincken, K.L., van Osch, M.J., Bisschops, R.H., van der Grond, J., 2004. Probabilistic segmentation of white matter lesions in MR imaging. *NeuroImage* 21 (3), 1037–1044.
- Andreasen, N.C., Arndt, S., Swayze II, V., Cizadlo, T., Flaum, M., O'Leary, D., Ehrhardt, J.C., Yuh, W.T., 1994. Thalamic abnormalities in schizophrenia visualized through magnetic resonance image averaging. *Science* 266 (5183), 294–298.
- Ashburner, J., 2000. *Computational Neuroanatomy* [PhD Thesis]. London: College London.
- Bilder, R.M., Wu, H., Chakos, M.H., Bogerts, B., Pollack, S., Aronowitz, J., Ashtari, M., Degreaf, G., Kane, J.M., Lieberman, J.A., 1994. Cerebral morphometry and clozapine treatment in schizophrenia. *J. Clin. Psychiatry* 55 (Suppl. B), 53–56.
- Bookstein, F.L., 2001. "Voxel-based morphometry" should not be used with imperfectly registered images. *NeuroImage* 14 (6), 1454–1462.
- Brett, M., Johnsrude, I.S., Owen, A.M., 2002. The problem of functional localization in the human brain. *Nat. Rev., Neurosci.* 3 (3), 243–249.
- Caviness Jr., V.S., Makris, N., Meyer, J., Kennedy, D., 1996. MRI-based parcellation of human neocortex: an anatomically specified method with estimate of reliability. *J. Cogn. Neurosci.* 8, 566–588.
- Cocosco, C.A., Zijdenbos, A.P., Evans, A.C., 2003. A fully automatic and robust brain MRI tissue classification method. *Med. Image Anal.* 7 (4), 513–527.
- Crespo-Facorro, B., Kim, J.J., Andreasen, N.C., O'Leary, D.S., Wiser, A.K., Bailey, J.M., Harris, G., Magnotta, V.A., 1999. Human frontal cortex: an MRI-based parcellation method. *NeuroImage* 10, 500–519.
- Csernansky, J.G., Joshi, S., Wang, L., Haller, J.W., Gado, M., Miller, J.P., Grenander, U., Miller, M.I., 1998. Hippocampal morphometry in schizophrenia by high dimensional brain mapping. *Proc. Natl. Acad. Sci. U. S. A.* 95 (19), 11406–11411.
- Dinov, I.D., Mega, M.S., Thompson, P.M., Lee, L., Woods, R.P., Holmes, C.J., Sumners, D.W., Toga, A.W., 2000. Analyzing functional brain images in a probabilistic atlas: a validation of subvolume thresholding. *J. Comput. Assist. Tomogr.* 24 (1), 128–138.
- Falkai, P., Bogerts, B., Greve, B., Pfeiffer, U., Machus, B., Folsch-Reetz, B., Majtenyi, C., Ovary, I., 1992. Loss of sylvian fissure asymmetry in schizophrenia. A quantitative post mortem study. *Schizophr. Res.* 7 (1), 23–32.
- Galaburda, A.M., Eidelberg, D., 1982. Symmetry and asymmetry in the human posterior thalamus: II. Thalamic lesions in a case of developmental dyslexia. *Arch. Neurol.* 39 (6), 333–336.
- Good, C.D., Johnsrude, I.S., Ashburner, J., Henson, R.N., Friston, K.J., Frackowiak, R.S., 2001a. Cerebral asymmetry and the effects of sex and handedness on brain structure: a voxel-based morphometric analysis of 465 normal adult human brains. *NeuroImage* 14 (3), 685–700.
- Good, C.D., Johnsrude, I.S., Ashburner, J., Henson, R.N., Friston, K.J., Frackowiak, R.S., 2001b. A voxel-based morphometric study of ageing in 465 normal adult human brains. *NeuroImage* 14 (1 Pt. 1), 21–36.
- Hammers, A., Allom, R., Koepp, M.J., Free, S.L., Myers, R., Lemieux, L., Mitchell, T.N., Brooks, D.J., Duncan, J.S., 2003. Three-dimensional maximum probability atlas of the human brain, with particular reference to the temporal lobe. *Hum. Brain Mapp.* 19 (4), 224–247.
- Kamber, M., Shinghal, R., Collins, D.L., Francis, G.S., Evans, A.C., 1995. Model-based 3-D segmentation of multiple sclerosis lesions in magnetic resonance brain images. *IEEE Trans. Med. Imag.* 14 (3), 442–453.
- Karas, G.B., Burton, E.J., Rombouts, S.A., van Schijndel, R.A., O'Brien, J.T., Scheltens, P., McKeith, I.G., Williams, D., Ballard, C., Barkhof, F., 2003. A comprehensive study of gray matter loss in patients with Alzheimer's disease using optimized voxel-based morphometry. *NeuroImage* 18 (4), 895–907.
- Kay, S.R., Fiszbein, A., Opler, L.A., 1987. The positive and negative syndrome scale (PANSS) for schizophrenia. *Schizophr. Bull.* 13, 261–276.
- Kikinis, R., Shenton, M.E., Iosifescu, D.V., McCarley, R.W., Saiviroonporn, P., Hokama, H.H., Robatino, A., Metcalf, D., Wible, C.G., Portas, C.M., Donnino, R.M., Jolesz, F.A., 1996. A digital brain atlas for surgical planning, model-driven segmentation, and teaching. *IEEE Trans. Vis. Comput. Graph.* 2, 232–241.
- Kim, J.J., Crespo-Facorro, B., Andreasen, N.C., O'Leary, D.S., Zhang, B., Harris, G., Magnotta, V.A., 2000. An MRI-based parcellation method for the temporal lobe. *NeuroImage* 11, 271–288.
- Kim, J.J., Yoon, T., Lee, J.M., Kim, I.Y., Kim, S.I., Kwon, J.S., 2003. Morphometric abnormality of the insula in schizophrenia: a comparison with obsessive-compulsive disorder and normal control using MRI. *Schizophr. Res.* 60 (2–3), 191–198.
- Kwon, J.S., Shin, Y.W., Kim, C.W., Kim, Y.I., Yoon, T., Han, M.H., Chang, K.H., Kim, J.J., 2003. Similarity and disparity of obsessive-compulsive disorder and schizophrenia in MR volumetric abnormalities of the hippocampus–amygdala complex. *J. Neurol., Neurosurg. Psychiatry* 74 (7), 962–964.
- Lawrie, S.M., Abukmeil, S.S., 1998. Brain abnormality in schizophrenia. A systematic and quantitative review of volumetric magnetic resonance imaging studies. *Br. J. Psychiatry* 172, 110–120.
- Lee, J.M., Yoon, U., Nam, S.H., Kim, J.H., Kim, I.Y., Kim, S.I., 2003. Evaluation of automated and semi-automated skull-stripping algorithms using similarity index and segmentation error. *Comput. Biol. Med.* 33 (6), 495–507.
- Lee, J.M., Kim, S.H., Jang, D.P., Ha, T.H., Kim, J.J., Kim, I.Y., Kwon, J.S., Kim, S.I., 2004. Deformable model with surface registration for hippocampal shape deformity analysis in schizophrenia. *NeuroImage* 22 (2), 831–840.

- Leemput, K.V., Maes, F., Vandermeulen, D., Suetens, P., 1999a. Automated model-based bias field correction of MR images of the brain. *IEEE Trans. Med. Imag.* 18 (10), 885–896.
- Leemput, K.V., Maes, F., Vandermeulen, D., Suetens, P., 1999b. Automated model-based tissue classification of MR images of the brain. *IEEE Trans. Med. Imag.* 18 (10), 897–908.
- Momenan, R., Rawlings, R., Fong, G., Knutson, B., Hommer, D., 2004. Voxel-based homogeneity probability maps of gray matter in groups: assessing the reliability of functional effects. *NeuroImage* 21 (3), 965–972.
- Nasrallah, H.A., Schwarzkopf, S.B., Olson, S.C., Coffman, J.A., 1990. Gender differences in schizophrenia on MRI brain scans. *Schizophr. Bull.* 16 (2), 205–210.
- Park, H.J., Levitt, J., Shenton, M.E., Salisbury, D.F., Kubicki, M., Kikinis, R., Jolesz, F.A., McCarley, R.W., 2004. An MRI study of spatial probability brain map differences between first-episode schizophrenia and normal controls. *NeuroImage* 22 (3), 1231–1246.
- Pitiot, A., Toga, A.W., Thompson, P.M., 2002. Adaptive elastic segmentation of brain MRI via shape-model-guided evolutionary programming. *IEEE Trans. Med. Imag.* 21 (8), 910–923.
- Rademacher, J., Galaburda, A.M., Kennedy, D.N., Filipek, P.A., Caviness, V.S., 1992. Human cerebral cortex: localization, parcellation, and morphometry with magnetic resonance imaging. *J. Cogn. Neurosci.* 4, 352–374.
- Rex, D.E., Ma, J.Q., Toga, A.W., 2003. The LONI pipeline processing environment. *NeuroImage* 19 (3), 1033–1048.
- Roland, P.E., Zilles, K., 1994. Brain atlases—a new research tool. *Trends Neurosci.* 17 (11), 458–467.
- Shapleske, J., Rossell, S.L., Woodruff, P.W., David, A.S., 1999. The planum temporale: a systematic, quantitative review of its structural, functional and clinical significance. *Brain Res. Rev.* 29 (1), 26–49.
- Shenton, M.E., Kikinis, R., Jolesz, F.A., Pollak, S.D., LeMay, M., Wible, C.G., Hokama, H., Martin, J., Metcalf, D., Coleman, M., et al., 1992. Abnormalities of the left temporal lobe and thought disorder in schizophrenia. A quantitative magnetic resonance imaging study. *N. Engl. J. Med.* 327 (9), 604–612.
- Suzuki, M., Nohara, S., Hagino, H., Kurokawa, K., Yotsutsuji, T., Kawasaki, Y., Takahashi, T., Matsui, M., Watanabe, N., Seto, H., et al., 2002. Regional changes in brain gray and white matter in patients with schizophrenia demonstrated with voxel-based analysis of MRI. *Schizophr. Res.* 55 (1–2), 41–54.
- Thompson, P., Mega, M., Toga, A., 2000. Disease-specific brain atlases. In: Mazziotta, J., Toga, A., Frackowiak, R. (Eds.), *Brain Mapping: The Disorders*. Academic Press, San Diego.
- Toga, A.W., Thompson, P.M., Mega, M.S., Narr, K.L., Blanton, R.E., 2001. Probabilistic approaches for atlas normal and disease-specific brain variability. *Anat. Embryol. (Berl)* 204 (4), 267–282.
- Tomaiuolo, F., MacDonald, J.D., Caramanos, Z., Posner, G., Chiavaras, M., Evans, A.C., Petrides, M., 1999. Morphology, morphometry and probability mapping of the pars opercularis of the inferior frontal gyrus: an in vivo MRI analysis. *Eur. J. Neurosci.* 11 (9), 3033–3046.
- Wang, L., Joshi, S.C., Miller, M.I., Csernansky, J.G., 2001. Statistical analysis of hippocampal asymmetry in schizophrenia. *NeuroImage* 14 (3), 531–545.
- Wilke, M., Schmithorst, V.J., Holland, S.K., 2003. Normative pediatric brain data for spatial normalization and segmentation differs from standard adult data. *Magn. Reson. Med.* 50 (4), 749–757.
- Woods, R.P., Grafton, S.T., Holmes, C.J., Cherry, S.R., Mazziotta, J.C., 1998a. Automated image registration: I. General methods and intrasubject, intramodality validation. *J. Comput. Assist. Tomogr.* 22 (1), 139–152.
- Woods, R.P., Grafton, S.T., Watson, J.D., Sicotte, N.L., Mazziotta, J.C., 1998b. Automated image registration: II. Intersubject validation of linear and nonlinear models. *J. Comput. Assist. Tomogr.* 22 (1), 153–165.
- Wright, I.C., Rabe-Hesketh, S., Woodruff, P.W., David, A.S., Murray, R.M., Bullmore, E.T., 2000. Meta-analysis of regional brain volumes in schizophrenia. *Am. J. Psychiatry* 157 (1), 16–25.
- Yoon, U., Lee, J.M., Kim, J.J., Lee, S.M., Kim, I.Y., Kwon, J.S., Kim, S.I., 2003. Modified magnetic resonance image based parcellation method for cerebral cortex using successive fuzzy clustering and boundary detection. *Ann. Biomed. Eng.* 31 (4), 441–447.
- Zijdenbos, A.P., Dawant, B.M., Margolin, R.A., Palmer, A.C., 1994. Morphometric analysis of white matter lesions in MR images. *IEEE Trans. Med. Imag.* 13 (4), 716–724.